Available online at www.sciencedirect.com
SCIENCE DIRECT®
Sensors and Actuators B 92 (2003) 37–43
SENSORS AND ACTUATORS B CHEMICAL
www.elsevier.com/locate/sensorb

Increasing the performance of high-pressure, high-efficiency electrokinetic micropumps using zwitterionic solute additives

David S. Reichmuth, Gabriela S. Chirica, Brian J. Kirby*

Microfluidics Department, Sandia National Laboratories, P.O. Box 969, MS 9951, Livermore, CA 94551, USA

Accepted 14 January 2003

Abstract

A zwitterionic additive is used to improve the performance of electrokinetic micropumps (EK pumps), which use voltage applied across a porous matrix to generate electroosmotic pressure and flow in microfluidic systems. Modeling of EK pump systems predicts that the additive, trimethylammoniopropane sulfonate (TMAPS), will result in up to a 3.3-fold increase in pumping efficiency and up to a 2.5-fold increase in the generated pressure. These predictive relations compare well with experimental results for flow, pressure and efficiency. With these improvements, pressures up to 156 kPa/V (22 psi/V) and efficiency up to 5.6% are demonstrated. Similar improvements can be expected from a wide range of zwitterionic species that exhibit large dipole moments and positive linear dielectric increments. These improvements lead to a reduction in voltage and power requirements and will facilitate miniaturization of micro-total-analysis systems (μTAS) and microfluidically driven actuators. Published by Elsevier Science B.V.

Keywords: Micropump; Electroosmosis; Zwitterion; Dielectric increment

1. Introduction

Micro-total-analysis systems (μTAS) have received a great deal of recent attention owing to their ability to improve the performance of chemical analysis systems by reducing footprint, reagent volumes, and electrical power needs. As a crucial component of μTAS research, micropumps have been investigated as a means to move fluids and actuate microscale mechanical components. Previous investigators have presented micropumps in a variety of formats, as reviewed in recent papers [1,2]. Electrokinetic micropumps (EK pumps) have been shown to generate pressures above 57 MPa (8000 psi) [3] or flow rates above 1 μl/min [2], making them attractive for miniaturization of HPLC systems [4], cooling of microelectronics, and actuation of microscale mechanical components [5].

EK pumps use electroosmosis in charged porous media to generate a pumping function. Electroosmotic flow (EOF) in porous matrices has been used in a variety of applications, including capillary electrochromatography [6,7], and microfluidic pumping [2,3,8]. EK pumps are ideally suited for μTAS, since they can straightforwardly meter the very low flow rates (nl/min or ml/min) that are typically used, and can generate high pressure (>10 MPa) required for chromatographic separations.

An EK pump is realized experimentally by applying voltage across a porous bed possessing a charged solid–liquid interface (Fig. 1). Electroosmosis due to the applied electrical field causes fluid flow and generates a pressure whose magnitude depends in part on the fluidic resistance of the channels downstream of the pump. Pump performance is dictated by substrate material and geometry as well as fluid properties. This paper presents the use of fluid additives to improve the pressure and flow rate performance of EK pumps. Important achievements include the demonstration of 156 kPa/V (22 psi/V) and 5.6% efficiency, both (to our knowledge) the highest performance reported for EK pumps.

2. Theory

In certain limits, EK pumps can often be modeled by straightforward equations. This section derives performance relations for EK pumps, with special attention to the effect of solutes. These relations will be used throughout the paper to illustrate the effects of uncharged, zwitterionic solute additives on pump performance.

EK pump performance parameters were first derived for capillaries using a Helmholtz double layer model [9], and later expanded to incorporate Gouy–Chapman double layers

* Corresponding author. Tel.: +1-925-294-2898; fax: +1-925-294-3020.
E-mail address: bjkirby@sandia.gov (B.J. Kirby).

0925-4005/03/$ – see front matter. Published by Elsevier Science B.V.
doi:10.1016/S0925-4005(03)00128-X

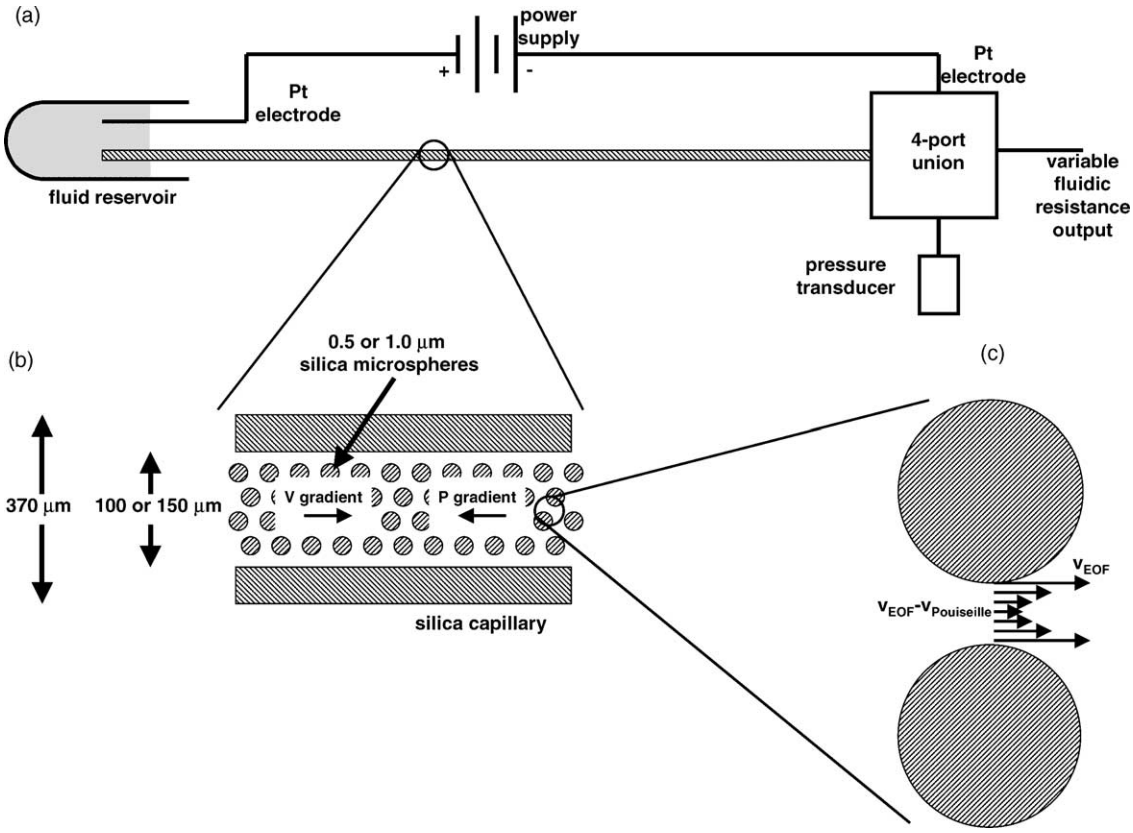

Fig. 1. EK pump operation and characterization. (a) Schematic of experimental setup. Voltage applied across a capillary packed with silica microspheres leads to flow and pressure generation. The fluidic resistance of the output channel controls the pressure and flow rate. Pressure is measured with a transducer and flow is measured by observation of meniscus motion through the output channel. (b) Expanded view of EK pump. Voltage gradient induces EOF from left to right; pressure gradient induces Pouiseille flow from right to left. (c) Expanded view of pores in between microspheres. Flow pattern is a linear superposition of solenoidal EOF from left to right and pressure-driven Poiseuille flow from right to left.

of finite size [10]. Building on early work, which considered simple geometries and often linearized the Poisson–Boltzmann equation [11], recent work has expanded this analysis to include detailed accounts of pore sizes and shapes [12] and fully explore the input parameter space [13] to evince nonlinear and limiting effects.

Here, we are concerned primarily with the relative performance change caused by adding solute to the pumped buffer, and anticipate working with high enough buffer concentrations (∼10 mM) that the Debye length [14] can be assumed small compared to the effective pore radius (∼100–200 nm). For this simple case, the electroosmotic flow (EOF) may be treated as uniformly proportional to the electric field throughout the pump medium.

Assuming a cylindrical capillary geometry with radius a and phenomenological zeta potential ζ (V), as well as a liquid with viscosity μ (Pa s), Stokes' flow equations can be combined with an electroosmotic forcing term to give the EOF profile as

$$u(r) = \frac{P_x}{4\mu}(a^2 - r^2) - \frac{\varepsilon\varepsilon_0\zeta E}{\mu} \quad (1)$$

where P_x (Pa/m) is the pressure gradient along the axis, r the radial position, and E (V/m) is the uniform electrical field. In this paper we use ε to denote the nondimensional dielectric constant such that the fluid permittivity is given by the product of the dielectric constant ε and the permittivity of free space ε_0. Eq. (1) can be used to derive a number of performance relations for EK pumps that consist of linear capillaries and operate in the thin double layer limit. Practical EK pumps consist not of linear capillaries but rather a porous bed; thus Eq. (1) can quantitatively treat porous media only if additional parameters (e.g., formation factors, porosity, tortuosity) are used to adapt the microchannel geometry to that of the porous bed. These additional parameters add multiplicative factors to Eq. (1) and the derived results to follow. However, the theory in this section is concerned primarily with the relative performance increase observed upon addition of specific fluid additives; thus the treatment for an idealized linear capillary system will be retained; it is simple and sufficient for this purpose. This derivation has been presented in [9], but is repeated here for clarity.

From Eq. (1) we can derive that the maximum pressure per volt generated in such a capillary (i.e., the pressure performance at zero net flow rate) is

$$\frac{\Delta P_{max}}{V} = \frac{8\varepsilon\varepsilon_0\zeta}{a^2} \quad (2)$$

where V is the applied voltage. As a practical example, we can use Eq. (2) to estimate that for a packed bed of 0.5 μm silica beads (effective pore radius $a \sim 100$ nm) and a fluid consisting of a 10 mM aqueous Tris (tris(hydroxymethyl)aminomethane hydrochloride) buffer ($\zeta \sim 60$ mV), the maximum pressure achieved will be 35 kPa/V (4.9 psi/V).

Expanding the microchannel model to consider an array of identical microchannels of length l and total open cross-sectional area A, the maximum flow rate generated per applied volt can be derived as

$$\frac{Q_{\max}}{V} = \frac{\varepsilon\varepsilon_0\zeta A}{\mu l} \tag{3}$$

Returning to the packed silica bead example and assuming the beads are packed into a 150 μm diameter cylindrical porous bed with a porosity of 0.33 and length of 5 cm, Eq. (3) gives $Q_{\max}/V = 0.3$ μl/min kV.

Since this flow is in the Stokes regime, the system is linear and a straightforward relationship for the flow rate or generated pressure can be derived from Eqs. (2) and (3):

$$Q = Q_{\max}\left(\frac{\Delta P_{\max} - \Delta P}{\Delta P_{\max}}\right) \tag{4}$$

Finally, we can define the efficiency as

$$\eta = \frac{Q\Delta P}{VI} \tag{5}$$

where VI is the applied electrical power and $Q\Delta P$ is the generated mechanical power. Differentiating Eq. (5) and inserting Eq. (4) leads to the conclusion that maximum efficiency is achieved at $P = 0.5P_{\max}$.

From Eqs. (2)–(5), design requirements for the substrate material, substrate porosity, solvent fluid, and dissolved species are clear. The substrate material affects the zeta potential ζ, and maximizing ζ will maximize pressure, flow rate, and thermodynamic performance. Silica surfaces give high wall potentials at neutral pH and above, and are a common material choice [2,3]. Choice of pore size directly affects pressure performance but does not affect flow rate. Solvents should be chosen to maximize permittivity and minimize viscosity. Water has typically been an attractive fluid for high pressure applications, due to its high dielectric constant ($\varepsilon \sim 81$, $\mu = 1$ mPa s at room temperature), while the addition of acetonitrile to aqueous pump fluids increases pumping rates, since its dielectric constant and viscosity ($\varepsilon \sim 37$, $\mu = 0.37$ mPa s) lead to a slightly better ε/μ ratio.

A minimum buffer concentration is often necessary for chemical analysis or synthesis. Here, we assume that a nominal buffer concentration is required, and that concentration leads to thin double layers. In this limit, addition of further charged species increases conductivity and power dissipation in the fluid, reducing efficiency and increasing unwanted thermal effects. Added counterions also reduce the zeta potential [15,16]. Hence, in the thin double layer limit, efficiency is approximately inversely proportional to concentration of charged species.

While small, uncharged solute additives do not significantly affect double layer thickness, wall zeta potential, or pH, they can have a large impact on the permittivity conductivity, and viscosity of the solution. In general, the dielectric constant of a dielectric electrolyte solution can be approximated using a linear dielectric increment $\mathrm{d}\varepsilon/\mathrm{d}C$:

$$\varepsilon(C) = \varepsilon(0) + \frac{\mathrm{d}\varepsilon}{\mathrm{d}C}C \tag{6}$$

where C is the concentration of solute and the linear dielectric increment is a property of the specific solute-solvent system. Normalizing these values, we can write

$$\varepsilon^* = 1 + \gamma_\varepsilon C \tag{7}$$

where $\varepsilon^* = \varepsilon/\varepsilon(0)$ and $\gamma_\varepsilon = (\mathrm{d}\varepsilon/\mathrm{d}C)/\varepsilon(0)$. Eq. (6) is rigorously valid only for infinitesimal concentrations but is typically accurate for practical concentrations, and will be shown later to be applicable up to 2.5 M for the solute considered in this paper.

The expected effect of zwitterionic additives follows directly from Eqs. (2)–(5) and can be expressed using the parameters defined in Eqs. (6) and (7). Upon addition of an uncharged additive, the EOF velocity changes linearly with the permittivity, leading to a change in pressure performance:

$$\frac{P_{\max}/V}{(P_{\max}/V)_0} = 1 + \gamma_\varepsilon C \tag{8}$$

Here, and in the following equations, the subscript 0 denotes the value at zero concentration. The change in EOF velocity similarly affects the maximum flow rate, but it is, offset by changes in the fluid viscosity:

$$\frac{Q_{\max}/V}{(Q_{\max}/V)_0} = \frac{1 + \gamma_\varepsilon C}{\mu^*} \tag{9}$$

where $\mu^* = \mu/\mu(0)$ is the normalized viscosity, whose functional form is left unspecified. Pressure and flow effects, combine with changes in conductivity to give the efficiency:

$$\frac{\eta}{\eta_0} = \frac{(1 + \gamma_\varepsilon C)^2}{\mu^*\sigma^*} \tag{10}$$

Here, $\sigma^* = \sigma/\sigma_0$ is the normalized conductivity. Eqs. (8)–(10) are valid only if double layers are thin, convective charge transport can be ignored, and permittivity changes linearly with concentration. A tacit assumption in Eqs. (8)–(10) is that the bulk values for permittivity and viscosity may be used to predict the electroosmotic velocity in the double layer. Hence, for these equations to be valid, the region near the wall in which the solution permittivity is drastically reduced must be small compared to the Debye length. For water, the bulk permittivity is generally accepted to apply outside of the first few monolayers at the surface. For the added zwitterionic species, their larger dipole moment implies that the region in which the local electric field leads to orientation effects on the permittivity will be larger. For this analysis, however, these effects are ignored; the success of this model in predicting EK pump

performance will justify our neglecting near-surface permittivity effects.

From Eqs. (8)–(10), it is clear that solutes with large γ_ε (e.g., a number of zwitterions) can greatly enhance EK pump performance. These zwitterions typically possess large inherent dipole moments. Because many zwitterionic solutes can be added at high molarity, they can have an enormous effect on the solution permittivity. This same effect is typically ignored for charged solutes in EK pump applications, since they are rarely used above 20 mM (for example, for sodium chloride, $d\varepsilon/dC = -13\,M^{-1}$ [17], and below 60 mM the effect on permittivity is less than 1%). Zwitterions with significant charge spacing can have large dipole moments (20–25 D), and their dielectric increment stems primarily from the additive effect of their dipole moments to the inherent dipole moment of the solvent. Many families of zwitterions (e.g., trialkylammonioalkane sulfonates, alkyl imidazole alkane sulfonates, alkyl pyridine alkane sulfonates) have large positive dielectric increments (>40 M^{-1}) in water, and are soluble above 1 M. These zwitterions, when added to aqueous pump solutions, lead to large permittivity increases and give the potential for improved pump efficiency, pressure, and flow. Trimethylammoniopropane sulfonate (TMAPS) is examined here, chosen for its high dielectric increment and commercial availability. TMAPS is known to have a $d\varepsilon/dC$ of $+52\,M^{-1}$ [18], is uncharged over a wide range of pH, and is soluble to 3.5 M.

3. Device fabrication and experimental setup

Packed capillary pumps were prepared using standard slurry packing techniques. An amount of 1 or 0.5 μm diameter nonporous silica microspheres (Duke Scientific, Palo Alto, CA) were suspended in water and pumped through capillaries (370 μm OD, 100 or 150 μm ID) at 57 MPa (8000 psi) using an HPLC pump (Isco 100DX, Lincoln, NE). The initial frit was produced by producing a paste of potassium or sodium silicate and Nucleosil silica particles (5 μm diameter, 1000 Å pore size) then drying and sintering the mixture inside the capillary end [19]. The second retaining frit was fabricated by sintering a section of the column after packing. All chemicals were purchased from Aldrich, except for TMAPS, which was purchased under the trade name Z1-Methyl (Waters, Milford, MA).

Fig. 1 diagrams the experimental setup used to characterize the EK pumps. The low-pressure end of the pump was immersed in the running solution and voltage was applied by a high-voltage power supply (Stanford Research Systems PS325, Sunnyvale, CA). The high pressure end of the pump was electrically grounded and connected fluidically to both a pressure transducer (Senso-Metrics SP70D, Simi Valley, CA) and an outlet with controlled fluidic resistance (infinite for P_{max}/V measurements, zero for Q_{max}/V measurements, approximately equal to the fluidic resistance of the pump for η measurements). Pressure was given by the transducer output, and flow rate was calculated from microscope observation of the motion of the liquid–air meniscus in a 149 μm ID capillary. Voltage and current were monitored using an electrometer (Keithley 614, Cleveland, OH), and data was acquired by a PC running LabView (National Instruments, Austin, TX).

Solution viscosities, necessary to predict flow rate performance, were inferred by using a syringe pump (Cole-Parmer 74900, Vernon Hills, IL) to induce a controlled 8.3 μl/min flow rate through a 1.3 m length of 53 μm ID capillary and observing the upstream pressure.

The effect of TMAPS on pump performance was evaluated by measuring flow, pressure, and efficiency of two EK pumps with solutions with varying TMAPS concentrations. One pump, denoted as pump A, consisted of a 150 μm diameter capillary packed with 1 μm silica beads; the second pump, denoted as pump B, consisted of a 100 μm diameter capillary packed with 0.5 μm silica beads.

4. Results

The effect of TMAPS concentration on EK pump performance was investigated in the maximum-pressure, maximum-flow, and maximum-efficiency limits. Measurements of viscosity and dielectric increment allow effects of TMAPS concentration to be compared to those predicted by theory. Fig. 2 shows the measured viscosities for 10 mM Tris buffers with varying TMAPS concentrations.

The maximum-pressure performance of the pump was measured by sealing the pump outlet to produce zero net mass flux through the pump. Tris buffers (pH 8.5, 10 μm) were used, and the effect of TMAPS was observed by measuring P_{max}/V for various TMAPS concentrations. At each concentration, equilibrium pressure was recorded as a function of several applied voltages, and the observed pressure vs. voltage curve was fit to a linear relationship, whose slope gives the pressure/voltage parameter from

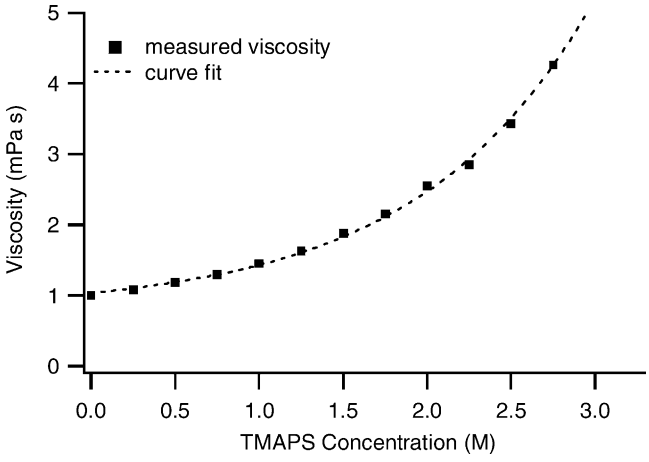

Fig. 2. Solution viscosity as a function of TMAPS concentration. An exponential curve fit ($0.244\exp[0.964C] + 0.792$) is used to phenomenologically fit the data.

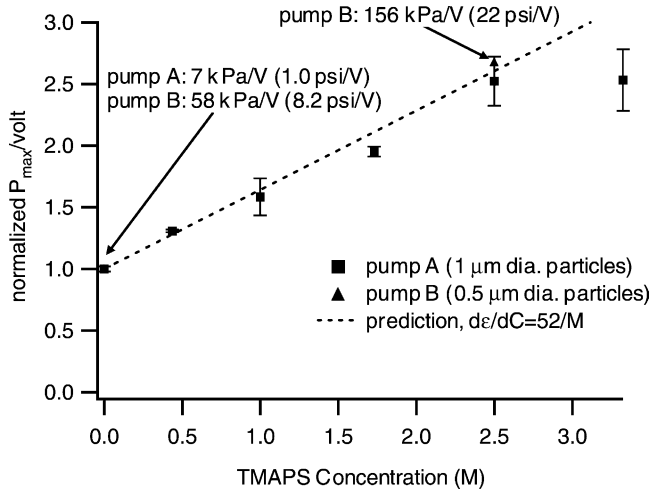

Fig. 3. Effect of TMAPS on maximum pressure per volt (P_{max}/V), measured at zero net mass flux. For this figure and Figs. 4–6, the buffer is 10 mM Tris with varying TMAPS concentrations, and results for each pump are normalized to the value obtained for that pump without TMAPS. The dashed line is a prediction based on water's dielectric constant of 81 and a linear dielectric increment of 52 M^{-1} [18]. Error bars indicate the standard deviation of the linear fit of the pressure vs. voltage curve at each concentration.

Eq. (2). Fig. 3 shows the pressure/voltage response normalized by the value observed without TMAPS, plotted as a function of the TMAPS additive concentration. Error bars indicate the standard deviation of the linear fit. The TMAPS additive caused up to a 2.5-fold increase in the observed P_{max}/V over the Tris buffer alone, leading to P_{max}/V results as high as 156 kPa/V (22 psi/V). The increase was linear up to 2.5 M TMAPS, and is consistent (8.7% RMS error) with a prediction using a linear model for dielectric constant (Eq. (8)). A least squares fit (Fig. 4) of the 0–2.5 M region gives an inferred dielectric increment of 47.6 M^{-1}. This is consistent with a report of 52 M^{-1} for TMAPS [18] and the value of 42.2 M^{-1} reported for a similar compound, triethylammoniopropane sulfonate [20].

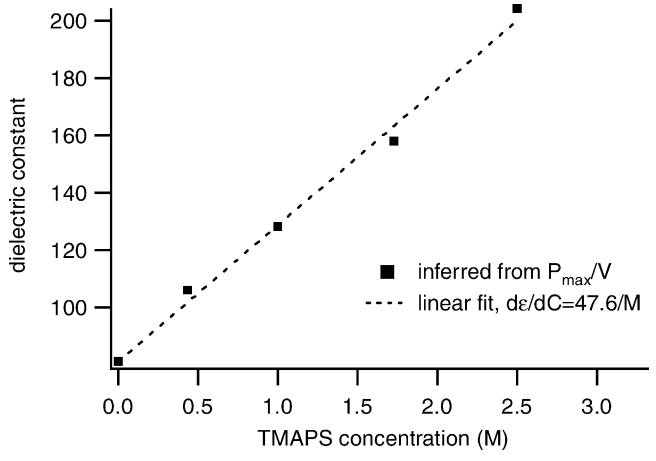

Fig. 4. Dielectric increment ($\delta\varepsilon/\delta\varepsilon = 47.6/M$) of TMAPS inferred from a linear fit of P_{max} data in over a concentration range of 0–2.5 M.

From Fig. 3, we can also observe that, while variation in fabrication can lead to changes in the absolute performance of individual pumps, these variations do not affect the relative impact of solute additives on performance. Inconsistencies in the quality of the packed bed lead to significant variations in individual pump performance: for example, using a Tris buffer with no TMAPS, the maximum pressure/voltage values for our 1 μm particle pumps have varied from 3.5 to 17.5 kPa/V (0.5 to 2.5 psi/V), and results from 0.5 μm particle pumps have varied from 14 to 40 kPa/V (2 to 10 psi/V). Thus the length scaling from Eq. (2) is observed on average but cannot be inferred from the relative P_{max}/V of the two pumps A and B used for this additive study. Pump A is a rather poorly performing pump, which presumably has a poorly ordered particle matrix and a number of packing defects, while pump B performs well and most likely has few defects. Despite these geometric variations, the effect of TMAPS is repeatable and, within the error of the measurements, equal for both pumps.

The effect of the TMAPS additive was also tested at the maximum flow rate (Q_{max}/V) by connecting the pump outlet to an open capillary. Flow rates were measured at several voltages and the slope of the linear relationship gives Q_{max}/V. Results as a function of TMAPS concentration are shown in Fig. 5 and compared to a prediction using Eq. (9) and the curve-fit viscosity from Fig. 2. The maximum flow rate increases at low concentrations, and is predicted to reach a maximum at 1 M TMAPS corresponding to a 20% increase over buffer alone. The maximum flow rate is observed to decrease beyond 1 M TMAPS, reaching a minimum at 3.3 M. The agreement (7.7% RMS error) between experiment and prediction is quite good.

Efficiency was calculated from pressure, flow, voltage, and current observations and the results are displayed in Fig. 6. Pump A was evaluated at $P = 0.47\,P_{max}$ ($\eta = 0.996\eta_{max}$), and

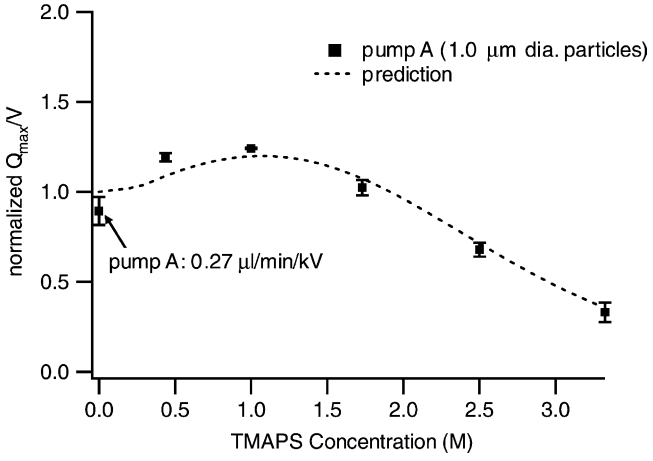

Fig. 5. Effect of TMAPS on Q_{max}/V, measured at zero pressure. Dashed line indicates predicted Q_{max}/V using experimental viscosity data and a dielectric increment of 52 M^{-1}. The absolute value for the experimental $(Q_{max}/V)_0$ has been chosen to best match the prediction. Error bars indicate the standard deviation of the linear fit of the flow rate vs. voltage curve at each concentration.

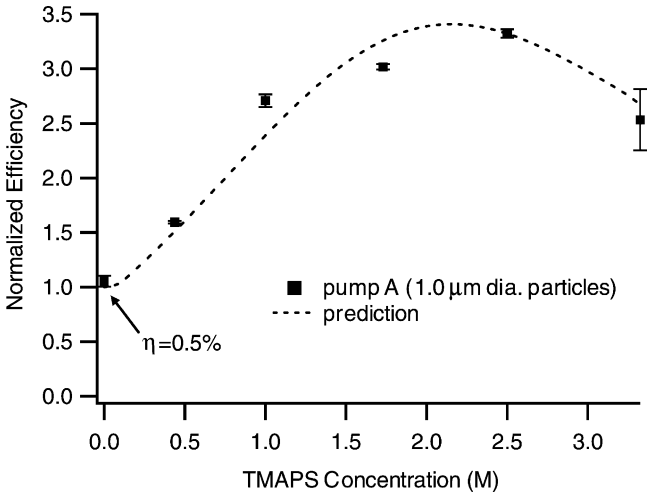

Fig. 6. Efficiency as a function of TMAPS concentration. Dashed line is a prediction Eq. (5) using experimental viscosity and conductivity data and a dielectric increment of 52 M^{-1}. The absolute value for the experimental η_0 has been chosen to best match the prediction. Error bars indicate the standard deviation of the measured efficiencies at various voltages for each concentration.

pump B was evaluated at $P = 0.65P_{max}$ ($\eta = 0.91\eta_{max}$). The prediction of Eq. (10) is shown for comparison. The addition of TMAPS increased the efficiency of the pump in the 0–2.5 M TMAPS range. Eq. (10) predicts a maximum efficiency at 2.2 M TMAPS, at which point the efficiency has increased by a factor of 3.3. The maximum observed efficiency was obtained with pump B at 2.5 M TMAPS, an efficiency of 5.6%. The predicted and observed curves agree quite well (8.4% RMS error).

5. Discussion

The permittivity increase caused by zwitterionic additives will significantly improve pump and actuator performance. The increase will allow the μTAS designer greater freedom in device construction. For a given pressure or flow requirements, improved pump performance implies that smaller voltages may be used, reducing substrate voltage holdoff requirements, electrolysis and bubble generation, and (in portable, miniaturized systems) high-voltage requirements. For a given voltage, increased pressure improves chromatographic performance, while increased flow improves the temporal response of EK-pump-driven actuators.

The applicability of the zwitterionic additive presented here depends on the system. We have used electroosmotic pumps to actuate monolithic polymer structures to perform microfluidic valving functions [5,21]. Because these devices isolate the pump fluid from the test fluid, additives have no impact on the system except through their effects on pump performance. For miniaturized HPLC systems that employ electroosmotic pumps, the effect of the additive on separation performance must be considered. TMAPS is currently marketed as an ion-pairing reagent for improving separation performance [22], although recent work has challenged claims regarding its effectiveness [18]. It is reasonable to expect in general that TMAPS will inhibit electrostatic interactions with surfaces; it is therefore inappropriate for ion-exchange chromatography but suitable for reversed-phase chromatography. A history of separation methods development using TMAPS already exists, and we expect that zwitterionic additives to EK-pumped separation buffers will find extensive use in the future.

The conclusions of this paper are clearly not limited to the zwitterion studied (TMAPS); a variety of zwitterions have large positive dielectric increments and high solubility and could be expected to have similar effects. Many of these zwitterions are aminopropane sulfonates or similar compounds that are marketed primarily as buffers for use near the amine pK_a; at mildly acidic pH these molecules are fully zwitterionic and can be used as uncharged additives.

The modeling presented here matches the data well, and can be expected to provide predictive capability for EK pumps with this and other zwitterionic additives. The model, though, requires several significant assumptions which limit its application. Most significant is the assumption that the electrical double layer is thin. Here, the Debye length (~3 nm) has been assumed thin as compared to the effective pore radius (~100–200 nm). Because of this, the permittivity affects pump performance only through its effect on electroosmotic velocities. For cases in which the Debye length is greater than 10% of the effective pore radius, the $\varepsilon^{1/2}$ dependence of the Debye length [14] leads to a secondary effect that cannot be ignored. Similarly, the thin double layer assumption ignores surface conductance and implies that maximum efficiency is observed at the lowest ionic strengths. This also breaks down, as the double layer becomes of significant size, since changes in double layer thickness changes the contribution of surface conductance to the current. Also of importance at lower ionic strengths is the convective component of the current, which can be ignored at high ionic strengths but must be inserted into Eq. (5) at low ionic strengths.

While the pressure and efficiencies observed with these pumps are to our knowledge the highest reported, clear paths exist to continuing improvements. Packing with smaller beads, while experimentally difficult, will lead to improved pressure/voltage results with the buffers used in this study. Improved efficiency may also be obtained simply by decreasing the buffer concentration so that the Debye length is approximately one-third of the effective pore size [10,13].

6. Conclusions

The effect on EK pump performance of adding TMAPS to the pumped fluid has been investigated. By increasing the permittivity of the solution, addition of up to 2.5 M TMAPS to the buffer multiplies the maximum pressure generated per volt by a factor up to 2.5. Up to a 20% increase in flow rate is

observed (at $C = 1$ M). Efficiency can be increased by a factor as high as 3.3, due to the permittivity increase as well as the conductivity decrease. With these improvements, pressures as high as 156 kPa/V (22 psi/V) and efficiencies of 5.6% have been demonstrated. Simple performance predictions have been derived using EOF relations for linear microchannel geometries with vanishingly thin double layers. Similar improvements should be observed with any of a wide variety of zwitterions with positive dielectric increments. We expect that these improvements will enable the production of more efficient and quickly actuated mechanical microdevices, facilitate miniaturization and portability of microchip-based HPLC systems, enable ultra-high pressure generation, and (through increases in efficiency) reduce electrolysis and bubble generation.

Acknowledgements

The technical expertise of R.F. Renzi is gratefully acknowledged. This work was supported by the Laboratory Directed Research and Development program at Sandia National Laboratories. Sandia National Laboratories is a multiprogram laboratory operated by Sandia Corporation, a Lockheed Martin Company, for the United States Department of Energy under contract DE-AC04-94AL85000.

References

[1] D.R. Reyes, D. Iossifidis, P.-A. Auroux, A. Manz, Micro total analysis systems, Anal. Chem. 74 (2002) 2623.
[2] S. Zeng, C.H. Chen, J.C. Mikkelsen Jr., J.G. Santiago, Fabrication and characterization of electroosmotic micropumps, Sens. Actuators B 79 (2001) 107.
[3] P.H. Paul, D.W. Arnold, D.J. Rakestraw, in: D.J. Harrison, A.V.d. Berg (Eds.), μTAS 98, Kluwer Academic Publishers, Dordrecht, 1998, 49 pp.
[4] P.H. Paul, D.W. Arnold, D.W. Neyer, K.B. Smith, in: A.V.d. Berg (Ed.), μTAS 2000, Kluwer Academic Publishers, Dordrecht, 2000, 583 pp.
[5] B.J. Kirby, T.J. Shepodd, F. Ernest, J. Hasselbrink, Voltage-addressable on/off microvalves for high-pressure microchip separations, J. Chromatogr. A 979 (2002) 147.
[6] J.H. Knox, I.H. Grant, Chromatographia 32 (1991) 317.
[7] D.J. Throckmorton, T.J. Shepodd, A.K. Singh, Electrochromatography in microchips: reversed-phase separation of peptides and amino acids using photopatterned rigid polymer monoliths, Anal. Chem. 74 (2002) 784.
[8] F.A. Morrison Jr., J.F. Oesterle, J. Sci. Ind. Res. 28 (1969) 284.
[9] J.F. Oesterle, Electrokinetic energy conversion, J. Appl. Mech. 31 (1964) 161
[10] J. Morrison, F.A., J.F. Oesterle, Electrokinetic energy conversion in ultrafine capillaries, J. Chemi. Phys., 43 (1965) 2111.
[11] C.L. Rice, R. Whitehead, Electrokinetic flow in a narrow cylindrical capillary, J. Phys. Chem. 69 (1965) 4017.
[12] D. Coelho, M. Shapiro, J.F. Thovert, P.M. Adler, Electroosmotic phenomena in porous media, J. Colloid Interf. Sci. 181 (1996) 169.
[13] S.K. Griffiths, R.H. Nilson, in: Y. Baba (Ed.), μTAS 2002, Kluwer Academic Publishers, Dordrecht, 2002, 133 pp.
[14] R.F. Probstein, Physicochemical Hydrodynamics, Wiley/Interscience, New York, 1994.
[15] A. Revil, P.A. Pezard, P.W.J. Glover, Streaming potential in porous media. 1. Theory of the zeta potential, J. Geophys. Res.-Solid Earth 104 (1999) 20021.
[16] P.J. Scales, F. Grieser, T.W. Healy, L.R. White, D.Y.C. Chan, Electrokinetics of the silica–solution interface: a flat plate streaming potential study, Langmuir 8 (1992) 965.
[17] R. Buchner, G.T. Hefter, P.M. May, Dielectric relaxation of aqueous NaCl solutions, J. Phys. Chem. A 103 (1999) 1.
[18] C.A. Lucy, M.A. Woodland, in: Proceedings of the 15th International Symposium on Microscale Separations and Analysis, The Swedish Chemical Society Analytical Division, Stockholm, Sweden, 2002.
[19] G. Chirica, V.T. Remcho, Silicate entrapped columns: new columns designed for capillary electrochromatography, Electrophoresis 20 (1999) 50.
[20] M. Galin, A. Chapoton, J.-C. Galin, Dielectric increments, intercharge distances and conformation of quaternary ammonioalkylsulfonates and alkoxydicyanothenolates in aqueous and trifluoroethanol solutions, J. Chem. Soc., Perkin Trans. 2 3 (1993) 545.
[21] E.F. Hasselbrink, T.J. Shepodd, J.E. Rehm, High pressure microfluidic control in lab-on-a-chip devices using mobile polymer monoliths, Anal. Chem. 74 (2002) 4913.
[22] M.M. Bushy, J.W. Jorgenson, Capillary electrophoresis of proteins in buffers containing high concentrations of zwitterionic salts, J. Chromatogr. 480 (1989) 301.

Biographies

David S. Reichmuth received a doctorate in 2002 and a master's degree in 1998 from the Chemical Engineering Department at the University of California, Berkeley. Dave is currently conducting research in microfluidics and laser-microfabrication.

Gabriela S. Chirica holds a PhD degree in Chemistry with a minor in Biochemistry from Oregon State University. She received her BS degree in chemical engineering in 1991 from University of Cluj Napoca, Romania. Her primary research interest is microscale separations.

Brian J. Kirby received a PhD in Mechanical Engineering from Stanford University in 2001. His interests include microfluidic transport, phase-separation polymerization, laser fabrication techniques, and nonlinear optics and spectroscopy.